

NANOINDENTATION AND NANOSCRATCHING OF HARD CARBON COATINGS FOR MAGNETIC DISKS

T.Y. TSUI*, G.M. PHARR*, W.C. OLIVER**, C.S. BHATIA***, R.L. WHITE***, S. ANDERS†, A. ANDERS†, and I. G. BROWN†

* Department of Materials Science, Rice University, Box 1892, Houston, TX 77251

** Nano Instruments, Inc., Box 14211, Knoxville, TN 37914

*** IBM Storage Systems Division, 5600 Cottle Road, San Jose, CA 95193

† Lawrence Berkeley Laboratory, Berkeley, CA 94720

The submitted manuscript has been authorized by a contractor of the U.S. Government under contract No. AC05-84OR21400. Accordingly, the U.S. Government retains a nonexclusive, royalty-free license to publish or reproduce the published form of this contribution, or allow others to do so, for U.S. Government purposes.

ABSTRACT

Nanoindentation and nanoscratching experiments have been performed to assess the mechanical properties of several carbon thin films with potential application as wear resistant coatings for magnetic disks. These include three hydrogenated-carbon films prepared by sputter deposition in a H₂/Ar gas mixture (hydrogen contents of 20, 34, and 40 atomic %) and a pure carbon film prepared by cathodic-arc plasma techniques. Each film was deposited on a silicon substrate to thickness of about 300 nm. The hardness and elastic modulus were measured using nanoindentation methods, and ultra-low load scratch tests were used to assess the scratch resistance of the films and measure friction coefficients. The results show that the hardness, elastic modulus, and scratch resistance of the 20% and 34% hydrogenated films are significantly greater than the 40% film, thereby showing that there is a limit to the amount of hydrogen producing beneficial effects. The cathodic-arc film, with a hardness of greater than 59 GPa, is considerably harder than any of the hydrogenated films and has a superior scratch resistance.

INTRODUCTION

Conventional magnetic hard disks are composed of multilayer thin films deposited on rigid substrates. During normal hard disk operation, a slider with active magnetic read-write elements flies above the disk and occasionally makes contact with it [1]. To prevent contact damage and wear in the relatively soft magnetic layer in which the data are stored, hard overcoats are usually employed in the disk structure.

A common material for overcoat protection is amorphous carbon, which is frequently prepared by sputter-deposition in a hydrogen atmosphere in a way which incorporates some hydrogen into the film. Hydrogenated-carbon films are generally much harder than their pure carbon counterparts, but exhibit mechanical properties which depend on the hydrogen content. One objective of the current report is to document the effects of hydrogen on the hardness, elastic modulus, and scratch resistance of several sputter-deposited, hydrogenated-carbon films.

A second objective of the paper is to compare the mechanical properties of hydrogenated films with those of a new carbon material prepared by cathodic-arc deposition. This relatively pure form of carbon has a hardness approaching that of diamond and is at least four times as hard as the best hydrogenated film studied here. As such, the material has great potential for application as a new hard disk overcoat material.

The mechanical properties were measured using nanoindentation and nanoscratching techniques described in detail in a previous report [2]. To facilitate comparison, all the films were deposited on silicon substrates to a thickness of approximately 300 nm.

PROCEDURE

The films examined in this study were prepared at two different laboratories. The hydrogenated-carbon films were made at the IBM Storage Systems Division, San Jose, CA, using sputter-deposition from a carbon source onto a stationary silicon substrate in a H₂/Ar

mixture. The hydrogen content was varied by controlling the hydrogen partial pressure in the sputtering chamber. Sputter pressures ranging from 5 to 10 mTorr were used, and the sputter power was adjusted to achieve a deposition rate of approximately 0.5 nm/sec. Three films, all 300 nm thick, were produced, containing 20, 34, and 40 atomic % hydrogen as measured using RBS techniques.

The cathodic-arc film was made at the Lawrence Berkeley Laboratory, Berkeley, CA, by cathodic-arc deposition with a 90° bent magnetic macroparticle filter and substrate pulse-biasing. Details of the deposition system and physical properties of the film are given elsewhere [3,4]. The cathodic-arc source was operated in a pulsed mode using a pulse duration of 5 ms, a frequency of 2 Hz, and a discharge current of 300 A. During immersion in the carbon plasma, the silicon substrate was repetitively pulse-biased at a negative voltage using a pulse duration time of 2 μ s and bias duty cycle of 25%. To promote film adhesion, a relatively high substrate bias of -2kV was applied in the initial stages of film growth, producing an atomically mixed interface of about 10 nm followed by a continued growth under the same conditions so as to form an amorphous carbon layer of about 30 nm thickness. The majority of the film was then grown on top of this layer at the lower substrate bias of -100V. Preliminary structural analysis using transmission electron microscopy (TEM) and electron energy loss spectroscopy (EELS) showed that the film contained a mixture of amorphous and nanocrystalline material with a sp³ bond content of about 85% [5]. Cross-sectional TEM revealed thin amorphous layers about 30 nm thick at both the substrate-film interface and the free surface [5].

Nanoindentation and nanoscratch tests were performed at Oak Ridge National Laboratory. The hardness, H, and elastic modulus, E, of each of the films were measured with a sharp Berkovich diamond indenter using the method developed by Oliver and Pharr [6]. The nanoscratch tests were conducted with a modified nanoindentation system incorporating sensors to measure the lateral forces on the indenter as the specimen was moved laterally underneath it [2]. A blunted Berkovich diamond oriented in a face-forward direction was used to make the scratches. As detailed elsewhere [2], during each nanoscratch experiment, the diamond tip was passed along the scratch track three separate times. The first pass, called the initial scan, was performed at the light load of 40 μ N and was used to map the slope and local topography of the specimen without damaging the surface. The surface profile determined in this scan was fitted to a ninth-order polynomial and subtracted from all scratch displacement data so that subtle features in the data could be observed. After the initial scan, a 1000 μ m long scratch was made by linearly ramping the load on the diamond from 0 to 100 mN as the specimen was laterally displaced at a velocity of 10 μ m/sec. A third scan, again at the constant light load of 40 μ N and referred to as the post-scratch scan, was then made to assess the changes in surface profile resulting from the scratch. From these measurements and optical examination of the scratch track, the critical load at failure, defined as the normal load at which permanent damage first occurred, was assessed. The coefficient of sliding friction as a function of position along the scratch track was also determined from the normal and lateral forces on the diamond.

RESULTS AND DISCUSSION

Nanoindentation

Nanoindentation test results for the films are shown in Figure 1, where the hardness and elastic modulus for each film are plotted as a function of indentation contact depth. Since the films were deposited on silicon, the hardnesses and moduli tend to converge at large contact depths towards the values for bulk silicon, 12 GPa and 163 GPa, respectively [7,8]. Values more representative of the films were obtained at small depths. Estimates of the film properties are summarized in Table I.

Perhaps the most notable feature in the H and E data is the extreme hardness of the cathodic-arc film; the 59 GPa value listed in the table is approximately 4 times that of the hardest of the hydrogenated films and is nearly 2/3 of the 90 GPa value for bulk crystalline diamond [9]. Moreover, the fact that there is no clear small-depth plateau in the hardness of the cathodic-arc material suggests that the nanoindentation measurements are not substrate independent. Thus, the

DISCLAIMER

This report was prepared as an account of work sponsored by an agency of the United States Government. Neither the United States Government nor any agency thereof, nor any of their employees, make any warranty, express or implied, or assumes any legal liability or responsibility for the accuracy, completeness, or usefulness of any information, apparatus, product, or process disclosed, or represents that its use would not infringe privately owned rights. Reference herein to any specific commercial product, process, or service by trade name, trademark, manufacturer, or otherwise does not necessarily constitute or imply its endorsement, recommendation, or favoring by the United States Government or any agency thereof. The views and opinions of authors expressed herein do not necessarily state or reflect those of the United States Government or any agency thereof.

DISCLAIMER

Portions of this document may be illegible in electronic image products. Images are produced from the best available original document.

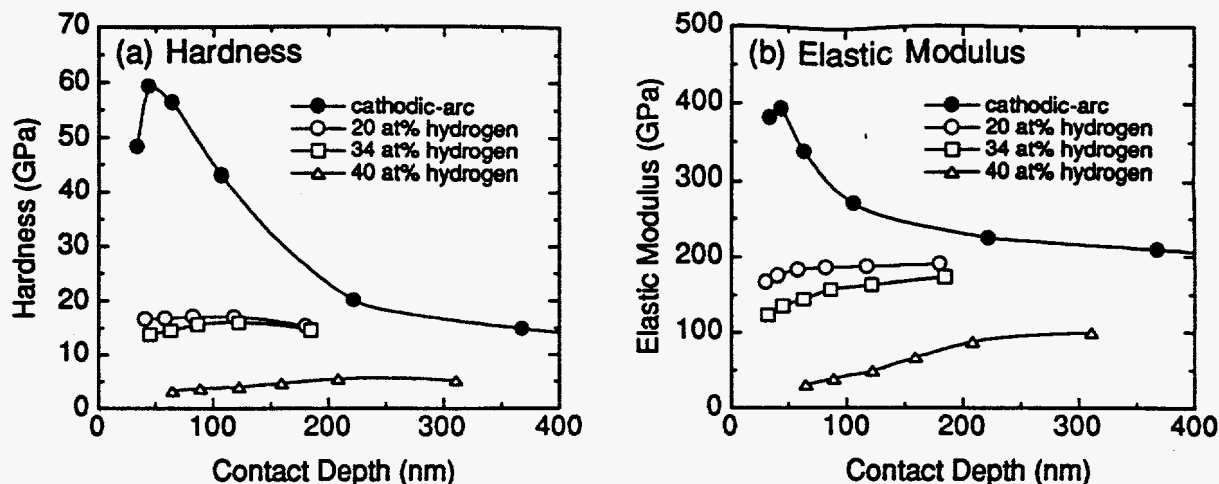


Figure 1. Nanoindentation measurements of (a) hardness and (b) elastic modulus.

true hardness of the film is probably even higher than the 59 GPa value and may approach that of diamond, consistent with the observation of at least some nanocrystalline material in the film [5]. The peak in H at small contact depths is believed to result from the amorphous surface layer observed in cross-sectional TEM [5]. Like the hardness, the elastic modulus shows a peak whose value of approximately 400 GPa also represents a lower limit. For comparison purposes, the modulus of bulk diamond is 1140 GPa [8].

Another notable feature in Figure 1 concerns the influence of hydrogen on the mechanical properties of the sputter-deposited films. The films containing 20% and 34% hydrogen have relatively high hardness and modulus, in the range $H=14-17$ GPa and $E=135-175$ GPa, but the properties of the 40% film, $H=3.3$ GPa and $E=31$ GPa, are considerably lower. The H and E values for the 40% film are in fact so low that one must question whether this is a hard-carbon material or a polymer. The properties of a sputter-deposited, hydrogen-free film were not measured in this study, but from previous work we know that such films typically have hardnesses of about 12 GPa. Thus, hydrogenation produces measurable increases in H , but there are also limits to the amount of hydrogen which is beneficial.

A question arises at this point as to what the optimum hardness and elastic modulus are for a protective overcoat film in hard disk applications. While it is generally held that high hardness is important, the role played by the modulus is not quite as clear. As a first step toward answering this question, it is useful to begin by assuming that overcoat films must be highly resistant to plastic deformation during contact events. This follows from the observation that many of the mechanisms of disk failure begin with or directly involve plastic deformation. In this regard, an analysis by Johnson which estimates the load, P_y , needed to initiate plastic deformation when a rigid sphere of radius, r , is pressed into contact with an elastic/plastic half-space, is useful [10]. Using Tabor's observation that the hardness of a material can be estimated as 3 times its yield strength [11], Johnson's analysis yields:

$$P_y = 0.78 r^2 \frac{H^3}{E^2} \quad (1)$$

This equation shows that the contact loads needed to induce plasticity are higher in materials with larger values of H^3/E^2 , i.e., the likelihood of plastic deformation is reduced in materials with high hardness and low modulus, with H^3/E^2 being the controlling material parameter.

Values of the plastic resistance parameter H^3/E^2 for the films examined in this study are included in Table 1. Clearly, the highest value is that for the cathodic-arc film, and in this regard, the cathodic-arc material is very attractive material for hard disk applications. It should be noted, however, that since the H and E values for the cathodic-arc film are lower limits and therefore only approximate, there is some uncertainty as to what the value of H^3/E^2 really is for the

Table I. Summary of nanoindentation and nanoscratch measurements.

Film Type	Hydrogen content (at %)	Thickness (nm)	Hardness (GPa)	Elastic Modulus (GPa)	$\frac{H^3}{E^2}$ (GPa)	Critical Load (mN)	Friction Coefficient
sputtered	20	300	17	175	0.16	39	0.15
sputtered	34	300	14	135	0.15	42	0.09
sputtered	40	300	3.3	31	0.04	17	0.06
cathodic-arc	0	320	>59	>395	~1.3	61	0.20

cathodic-arc film. For the hydrogenated-carbon films, the 20% and 34% films should be equally resistant to plasticity based on the H^3/E^2 comparison and significantly better than the 40% film.

Nanoscratch Tests

Nanoscratch tests were conducted to examine the general scratching behavior of the films and quantify the scratch resistance for purposes of materials comparison. A complete set of nanoscratch test results for the cathodic-arc film and the hardest of the hydrogenated films (20% hydrogen) are included in Figure 2. Each set of data includes an optical micrograph of the scratch with arrows marking the beginning and end of the scratch track along with a corresponding plot of the vertical displacements of the diamond during the initial scan, the load-ramped scratch, and the post-scratch scan. It should be recalled that the initial scan profiles the unscratched surface, and the post-scratch scan is used to determine the surface damage caused by the scratch. The displacements for each of the three passes have been corrected to account for the slope and topography of the surface by subtracting from them the displacements measured in the initial scan, and for this reason, the initial scan appears as a flat line. Note that negative displacements correspond to the scratch tip being pushed into the material, and positive displacements, which appear only in the post-scratch scan, indicate that the surface has blistered outward or that debris has accumulated in the scratch track. Values for the apparent friction coefficients are also included in the plots. The friction coefficients listed in Table I were obtained from such plots by choosing the value just prior to film failure.

Fig. 2a shows the nanoscratching behavior of the 20% hydrogenated-carbon film. The scratch can be divided into three regions based on differences in the appearance of the scratch track. Starting from the left and moving to the right, the first region is defined by the first 380 μm of the scratch. In this region, the scratch is extremely smooth and shallow, in fact, so shallow that it can be optically resolved in places only with differential interference contrast. Exactly how shallow the scratch is may also be seen by comparing the post-scratch scan to the initial scan; on the relatively gross normal displacement scale plotted in the figure, the two scans are virtually indistinguishable for the first 380 μm . A closer examination revealed that there is no remnant trace of the scratch in the left-hand portion of this region, corresponding to fully recovered elastic contact. Thus, scratching in the first region may be characterized as fully elastic followed by smooth elastic/plastic ploughing in which most of the normal displacement is recovered as the diamond passes by.

The second region of the 20% hydrogenated-carbon film scratch extends from 380 to 550 μm . In this region, the film blisters by delamination at the film/substrate interface. The blistering may be observed in the optical micrograph and is also apparent in the post-scratch scan, which shows the surface to be uplifted at numerous places in this region. Given that blistering is not desirable in hard disk applications, the load at the beginning of this region, 39 mN, is defined as the critical load for film failure. It is also notable that there is a subtle change in the rate of increase in the coefficient of friction at the beginning of the second region (see Fig. 2a) which can be used to define the onset of delamination.

The third and final region of the scratch in the 20% hydrogenated-carbon film begins at 550 μm and extends to the end of the scratch. It is marked by an abrupt change in the scratch

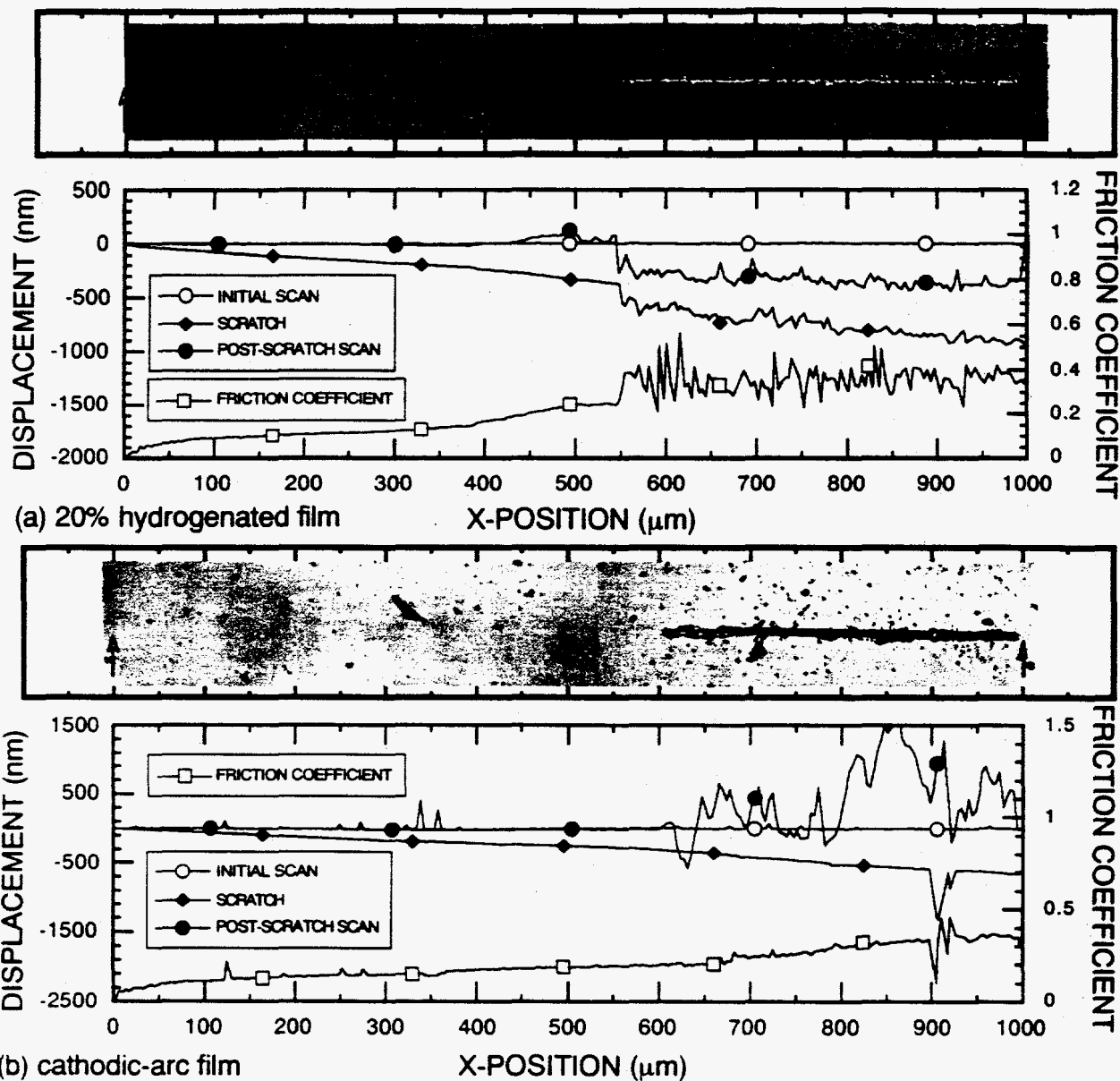


Figure 2. Optical micrographs of scratch tracks and scratch test results for: (a) the 20% hydrogenated-carbon film, and (b) the cathodic-arc carbon film.

displacement, as well as a substantial increase in the coefficient of friction. Examination of the optical micrograph reveals a large amount of small particle debris surrounding the scratch in this region, suggesting massive brittle fragmentation of the film. The post-scratch trace shows that the depth of fragmentation at the beginning of the third region is very close to the 300 nm film thickness, thus indicating complete failure and removal of the film. The overall picture which emerges is that the 20% hydrogenated film remains intact and is resistant to scratch damage at loads up to 39 mN, but increasing the load further causes the film to fail, first by delamination and blistering and then by massive brittle fragmentation.

The behavior of the cathodic-arc film is somewhat different, since as shown in Fig. 2b, only two distinct regions are observed. The first extends from 0-600 μm and is characterized by elastic contact followed by smooth elastic-plastic ploughing with nearly fully-recoverable normal displacements. At the 600 μm mark, however, corresponding to a load of 61 mN, failure begins abruptly by brittle fragmentation in the film and substrate. The brittle fragmentation is generally similar to that of the 20% hydrogenated film, but differs in that the debris particles are fewer in number and larger in size. More significantly, the critical failure load, 61 mN, is more than 50%

higher than that of the 20% hydrogenated film, thus indicating a significant increase in scratch resistance.

The critical failure loads for all four films are summarized in Table I. Using the critical load as a parameter for quantitatively assessing the scratch resistance of the materials, the cathodic-arc film is clearly the best, followed by the 34% and 20% hydrogenated films, while the 40% film is relatively poor. Examination of Table I also shows that the critical loads rank in an order which correlates reasonably well with the plastic resistance parameter, H^3/E^2 , possibly suggesting a correlation between film failure in the ramped-load scratch test and the onset of plastic deformation in the film.

CONCLUSION

In conclusion, the limited results obtained here suggest that cathodic-arc carbon may offer significant advantages over conventional sputter-deposited, hydrogenated carbon as a protective overcoat material in hard disk applications. The relative values of the hardness and modulus of cathodic-arc carbon make it significantly more resistant to plastic deformation during contact, as shown in ramped-load scratching experiments. For sputtered films, the hardness is increased by hydrogenation, but there is a limit to the amount of hydrogen producing beneficial effects. For the processing conditions used here, the 20% and 34% films exhibit higher hardness and better scratch resistance than the 40% film.

ACKNOWLEDGMENTS

This research was sponsored by the Advanced Research Projects Agency as a part of the National Storage Industry Consortium program in Ultra High Density Recording; by the Division of Materials Sciences, U.S. Department of Energy, under contract DE-AC05-84OR21400 with Martin Marietta Energy Systems, Inc. and through the SHaRE Program under contract DE-AC05-76OR00033 with the Oak Ridge Institute for Science and Technology; and by the U.S. Department of Energy, Division of Advanced Energy Projects, under contract No. DE-AC03-76SF00098.

REFERENCES

1. S. Chandrasekar and Bharat Bhushan, *J. Tribology* **112**, 1 (1990).
2. T.Y. Tsui, G.M. Pharr, W.C. Oliver, Y.W. Chung, E.C. Cutiongco, C.S. Bhatia, R.L. White, R.L. Rhodes and S.M. Gorbatskin, in Thin Films: Stresses and Mechanical Properties V, edited by S.H. Baker et al. (*Mater. Res. Soc. Proc.* **356**, Pittsburgh, PA), in press.
3. A. Anders, S. Anders, and I.G. Brown, *Plasma Sources Sci. Technol.* **4**, 1 (1995).
4. S. Anders, A. Anders, I.G. Brown, B. Wei, K. Komvopoulos, J.W. Ager, III, and K.M. Yu, *Surf. Coat. Technol.* **68/69**, 388 (1994).
5. G.M. Pharr, D.L. Callahan, S.D. McAdams, T.Y. Tsui, S. Anders, A. Anders, J.W. Ager III, I.G. Brown, C.S. Bhatia, S.R.P. Silva, and J. Robinson, submitted, *Applied Phys. Lett.*
6. W.C. Oliver and G.M. Pharr, *J. Mater. Res.* **7**, 1564 (1992).
7. G.M. Pharr, W.C. Oliver, and D.R. Clarke, *J. Elec. Mater.* **19**, 881 (1990).
8. G. Simmons and H. Wang, Single Crystal Elastic Constants and Calculated Aggregate Properties: A Handbook, 2nd ed. (MIT Press, Cambridge, MA, 1971).
9. C.A. Brookes, in The Properties of Diamond, edited by J. E. Field (Academic Press, New York, NY, 1979), pp. 383-402.
10. K.L. Johnson, Contact Mechanics, 1st ed. (Cambridge University Press, Cambridge, UK, 1985), p. 155.
11. D. Tabor, The Hardness of Metals, 1st ed. (Oxford University Press, Oxford, UK, 1951).